

CHAPTER 8

THERMAL EXPANSION

“Absence of evidence is not evidence of absence.”
M Rees

8.1 THERMAL REQUIREMENTS

When measuring the length of a length bar in the interferometer there is a potentially large source of error due to the fact that the bars are made of steel, which has a linear coefficient of thermal expansion of approximately $10.7 \times 10^{-6} \text{ K}^{-1}$. This means that the length of the bar will vary with temperature and hence must be referred to a standard temperature. Currently the standard reference temperature for metrological laboratories [1] is $20 \text{ }^\circ\text{C}$. Thus there two options for the measurement of length bars:

- (1) measure the length of the bar at exactly $20 \text{ }^\circ\text{C}$
- (2) measure the length of the bar at some other temperature and correct the measured length to $20 \text{ }^\circ\text{C}$ by using a value of the linear thermal expansion coefficient, α .

Both of these options require accurate measurement of temperature, in (1) to be sure that the bar is at exactly $20 \text{ }^\circ\text{C}$, and in (2) to apply a correction for the departure of temperature from $20 \text{ }^\circ\text{C}$.

The problem with option (1) is that it is difficult to stabilise the temperature of all the bars in the interferometer at exactly $20 \text{ }^\circ\text{C}$. Stable temperature conditions usually require good thermal conductivity (in this case of the air in the chamber) and a suitable reference temperature standard such as a melting point or a triple point. In the International Temperature Scale of 1990 (ITS90) [2] the nearest reference temperatures are at the triple point of water ($0.01 \text{ }^\circ\text{C} \pm 0.0005 \text{ }^\circ\text{C}$) and the melting point of gallium ($29.7646 \text{ }^\circ\text{C} \pm 0.005 \text{ }^\circ\text{C}$). These are not sufficiently close to $20 \text{ }^\circ\text{C}$ to allow accurate temperature stability at $20 \text{ }^\circ\text{C}$.

The problem with option (2) is that, according to the standards for gauge blocks and length bars, the coefficient of expansion for steel gauge blocks and length bars can vary, or is not defined:

<i>“the generally accepted value ... for steel is 11.5 parts in a million per degree Celsius”</i>	(BS 4311 - metric gauge blocks)
[no mention]	(BS 888 - imperial gauge blocks)
<i>“in the temperature range 10 °C to 30 °C shall be $(11.5 \pm 1.0) \times 10^{-6} \text{ K}^{-1}$”</i>	(DIN 861 - metric gauge blocks)
<i>“shall be within the limits $(11.5 \pm 1.0) \times 10^{-6}$ per degree Celsius”</i>	(ISO 3650 - metric gauge blocks)
[no mention]	(BS 5317 - metric length bars)
[no mention]	(BS 1790 - metric & imperial length bars)

There is increased awareness of the importance of the coefficient of thermal expansivity, as reflected in the wording of the latest British Standard [3] for gauge blocks:

“It is essential for gauge block manufacturers to use a grade and quality of material which is consistent and to control the processes of manufacture to enable the coefficient of expansion, within the temperature range 10 °C to 30 °C, to be within a tolerance of $\pm 0.5 \times 10^{-6}$ per °C of its stated value.”

Hence α may vary between 10.5 to 12.5 $\times 10^{-6} \text{ K}^{-1}$ between length bars in the same set (since they are often manufactured at different times from different batches of material) or by $\pm 0.5 \times 10^{-6} \text{ K}^{-1}$ for gauge blocks manufactured to the latest version of BS 4311. The different depth of hardening of bars may also lead to a variation, since short bars are hardened throughout their length whereas longer bars are hardened only partially. According to BS 5317:

“25 mm bars shall be hardened throughout their length. Bars over 25 mm up to and including 125 mm shall be hardened either throughout their length or at the ends only for a distance of not less than 4 mm. Longer bars shall be hardened at the ends only for a distance of about 6 mm and not less than 4 mm from each end.”

The hardened and un-hardened materials have different thermal expansion coefficients and hence the bulk average coefficient will depend on the length of the hardened zone, all other factors being equal.

Because of these variations and the emerging requirements from customers for higher accuracy length bar calibrations for length bars which may be used at temperatures other than 20 °C, it was decided that the interferometer would measure the length of bars at a temperature close to 20 °C (the final figure achieved is 20 °C \pm 0.03 °C) and correct the length to 20 °C using a nominal value of α . For the highest accuracy measurements, the interferometer would also operate as a dilatometer, *i.e.* it would

measure the lengths of bars at different temperatures over the range from 20 °C to 30 °C and thus derive an accurate value of α which could be used to accurately correct measured lengths to 20 °C or other temperatures.

8.2 TEMPERATURE CONTROL SYSTEM

Options considered for the temperature control of the interferometer included resistive heating wires, Thermofoil [4] heaters, Peltier effect devices and temperature-controlled flowing fluids. On grounds of cost, ease of use and ability to cool as well as heat, the design chosen was that of temperature-controlled water flowing in pipes inside the interferometer. A commercial temperature-controlled water bath and circulator was chosen to control the temperature of the water and to pump it around the pipes.

The baseplate of the interferometer is mounted on insulating nylon supports spaced at every 100 x 100 mm square. A copper pipe (8 mm diameter) is held against the bottom of the baseplate using steel clips. The pipe is wound into a spiral, shown in figure 8.1, with the pipe doubled-back against itself. The reason for this spiral is that when heat is being supplied to the chamber, the cooler return water runs alongside the hotter inflowing water. The coolest water outflow is next to the hottest inflow, thus the net temperature of flowing water at any point along the piping is approximately constant and equal to the mean of the inflow and outflow temperatures. There is a similar spiral of copper piping in the lid, which is held against the aluminium surface of the inside of the lid. Insulation material is used in the lid and against the side walls of the chamber and the interferometer is operated inside a temperature controlled laboratory (20 °C \pm 0.2 °C).

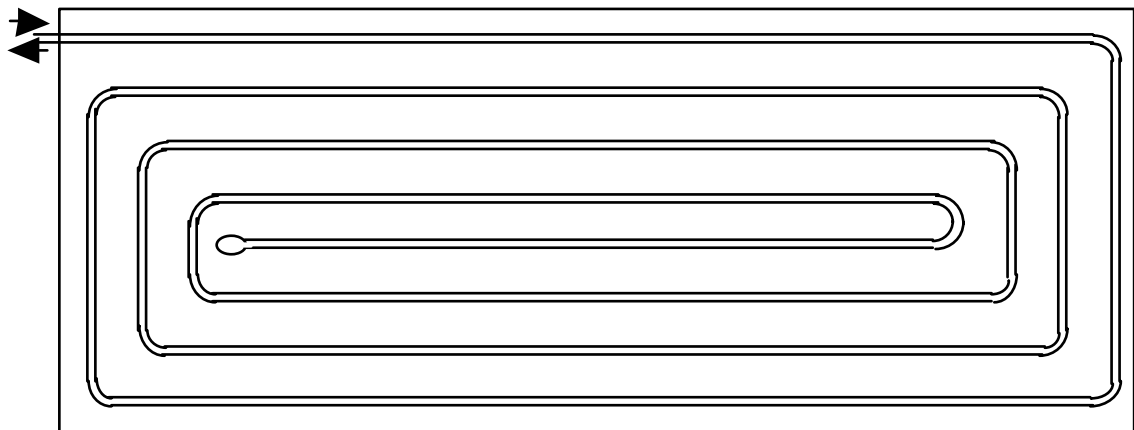


Figure 8.1 - Spiral of pipework on lid and baseplate

The water circulator is a Haake F3-CH unit which uses proportional-integral-derivative (PID) control to control a heater and refrigeration unit. The input signal for the controller is the temperature of a PRT placed in thermal contact with the baseplate, near the corner where the pipes are connected. The water flow from the Haake is split into two, one of which flows into the pipe in the lid, the other flows (via a valve) into the pipe below the baseplate. The accuracy of the Haake temperature control circuit is $\pm 0.02\text{ }^{\circ}\text{C}$, though any small temperature fluctuations will be integrated out by the thermal mass of the water and the chamber. The water flow rate is approximately $15\text{ litres min}^{-1}$. The Haake uses both a 1 kW heater and a 0.4 kW refrigerator, operating in push-pull mode with the heater under PID control. A front panel control allows selection of the set-point temperature in $0.1\text{ }^{\circ}\text{C}$ steps. The range of the temperature controller is dependent on the heat exchange liquid used. For water, the temperature is limited to the range $0\text{ }^{\circ}\text{C}$ to $60\text{ }^{\circ}\text{C}$ for safety requirements.

Initial experiments showed that the temperature inside the chamber was not uniform (at temperatures away from $20\text{ }^{\circ}\text{C}$). It was discovered that the temperature of the (unheated) side walls of the chamber were a few degrees cooler than the baseplate which was hotter than the lid. To solve this, three modifications were made. Firstly, the level of insulation was increased. A 50 mm thick box of Celotex™ Thermal Sheathing [5] was built around the interferometer, sitting on the edge of the optical table. Secondly, the water flow in the pipe below the baseplate was reduced, until the temperatures of the baseplate and lid were within $0.1\text{ }^{\circ}\text{C}$ of each other. Thirdly, heat shields were mounted on the edges of the baseplate - these are thin sheets of sand-blasted aluminium which are heated by conduction from the baseplate. These ‘shield’ the inside of the interferometer from the cooler side walls. (These can be seen in figure 3.25). Figure 8.2 shows the heating/cooling/insulation of the interferometer.

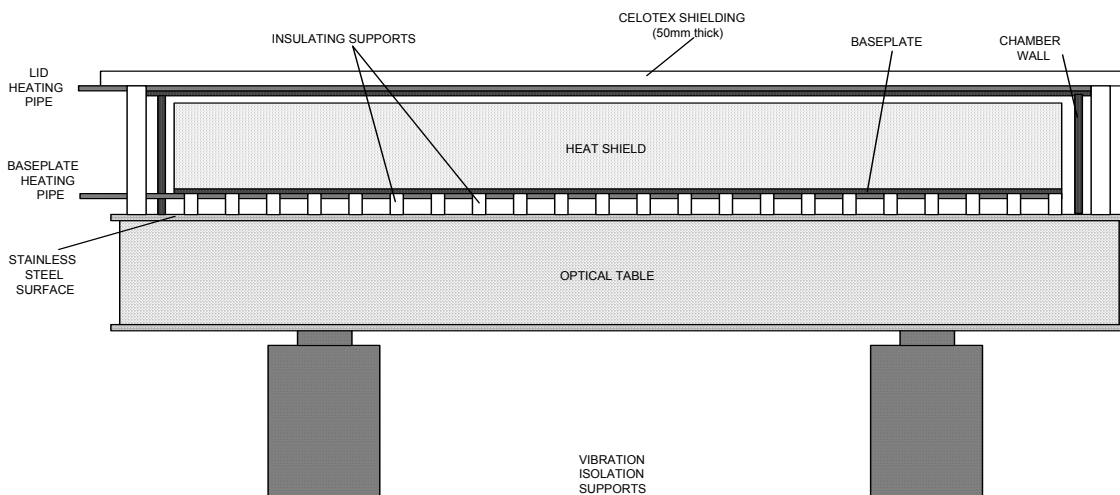


Figure 8.2 - Heating, cooling and insulation of interferometer

The non-uniform temperature caused turbulence and convection of the air inside the chamber leading to refractive index variations which distorted the fringes, making length measurement difficult and inaccurate. After balancing the temperatures of the top and bottom panels, an acceptable level of temperature homogeneity was achieved in both the lengths bars and the air inside the chamber. Details of the verification of this temperature homogeneity and an assessment of residual inhomogeneity are given below. There is a period of convection during the heating/cooling phase after a new set-point temperature is selected, but as the air reaches this temperature and the temperatures stabilise, no turbulence is visible. The video images show straight, stable fringes and the measurements of flatness and parallelism are similar to those made at 20 °C, showing that there is no distortion of the faces of the bar. If the chamber is opened whilst at a raised temperature, the fringes become distorted due to turbulence and thermal distortion of the platen due to the thermal shock

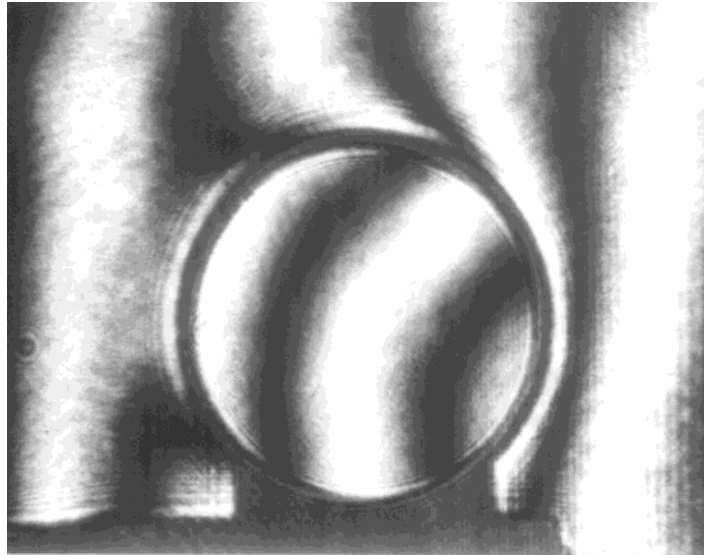


Figure 8.3 - Fringe distortion due to opening of chamber at raised temperature

8.3 TEMPERATURE MEASUREMENT SYSTEM

8.3.1 PRTs and resistance bridge details

All the temperatures inside the chamber are measured using 4-wire miniature platinum resistance thermometers (PRTs) conforming to standard DIN 43760 (1980) [6] and having resistance values within $\pm 0.01\%$ of those specified in that standard at 0 °C (referred to as “1/10 DIN” tolerance). These devices consist of a small coil of pure platinum wire

which has been manufactured by drawing platinum through a small sapphire or diamond die. The coil is suspended in a ceramic housing and has four pure platinum electrodes connected, two to either side of the coil, forming a standard four-terminal resistor. The resistance of the PRT is nominally 100 Ω at 0 $^{\circ}\text{C}$, rising to approximately 107.8 Ω at 20 $^{\circ}\text{C}$. The ceramic is bonded into a stainless steel sheath, 3 mm diameter and 25 mm long. Four thin wires, individually insulated and 2 m long are connected to the platinum leads. These wires are fed into 2 m long silicon tubing, terminated in a four-terminal LEMO plug. The plugs are inserted into feedthrough connectors in the chamber wall, which in turn are connected to the resistance bridge using individual BNC cables, two per PRT. These cables are designated the Potential (P) and Current (C) connections for the PRT. One cable is used to measure the voltage drop across the PRT when the other cable is supplying a current of 0.2 mA. The self-heating effect of the current in the PRT is approximately 1 - 2 mK, but is taken into account during the calibrations of the PRTs (see § 8.3.2).

The resistance bridge determines the ratio of the resistance of the PRT to the resistance of an internal temperature-controlled standard resistor. The bridge is calibrated using an external 100 Ω standard resistor, which is calibrated against standards traceable to the NPL realisation of the ohm, using the quantum Hall resistance (see § 7.3.2, § 10.4.2 and § 10.4.7 for further details of the resistance bridge). The PRTs are connected to the bridge via a 15-way selector switch, which is controlled by commands sent to the bridge's IEEE interface from the control computer.

8.3.2 Calibration of PRTs

The PRTs are calibrated by Temperature Section, NPL. To reproduce the conditions in which they are used, the calibration is performed with them connected to a similar resistance bridge, using the same connectors as used in the interferometer. The PRTs are calibrated by measuring their resistances at the triple point of water (0.01 $^{\circ}\text{C}$, $\pm 0.000 5$ $^{\circ}\text{C}$) and the melting point of gallium (29.7646 $^{\circ}\text{C} \pm 0.000 5$ $^{\circ}\text{C}$). These are two of the recommended fixed points of the International Temperature Scale (1990). The calibrations are carried out using the same current as in the interferometer. Thus the effects of self-heating are negated. From the values of the resistances measured at these two points, the corresponding ITS-90 coefficients can be calculated.

Periodically, the PRTs are checked by measuring their resistances at the triple point of water using a triple point cell.

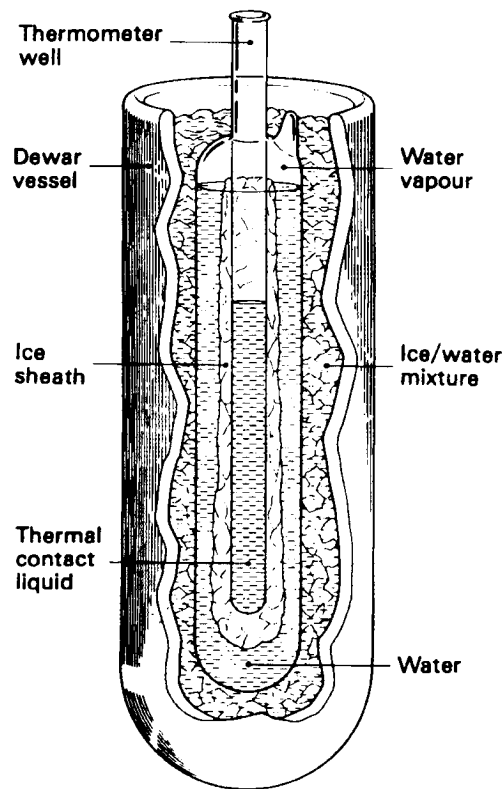


Figure 8.4 - Triple point of water cell used for temperature calibrations

8.3.3 Temperature measurements using ITS-90

From the triple point of equilibrium hydrogen at 13.8033 K to the freezing point of silver at 961.78 °C, the ITS-90 is realised using PRTs. The measurements of temperature are based on reference functions describing the behaviour of the resistance of standard PRTs, and deviation equations describing the departure of a PRT from this reference, measured during calibration. The functions are written in terms of the resistance ratios of the measured resistance at a particular temperature to the resistance at the triple point of water.

$$W = \frac{R(T)}{R(0.01^\circ\text{C})} \quad (8.1)$$

For the range of temperatures above 0 °C, the deviation equation is

$$W - W_{ref} = a(W - 1) + b(W - 1)^2 + c(W - 1)^3 + d \{W - W(660.323^\circ\text{C})\}^2 \quad (8.2)$$

where W and W_{ref} are the thermometer and reference resistance ratios, respectively. The determination of the coefficients a , b , c and d is made from measurements at various freezing points. The ITS-90 guidelines also permit single-point determinations with $b = c = d = 0$, and the measurement performed at the melting point of gallium (or the freezing

point of indium). This still requires determination of $R(0.01\text{ }^\circ\text{C})$ and hence is really a two-point calibration which results in a measured value of $R(0.01\text{ }^\circ\text{C})$ and a determined value of a .

To calculate a temperature, based on a measurement of resistance of a PRT requires the following procedure. W_{ref} is calculated from the deviation equation, using values of W and a . The appropriate reference function is then used to calculate the temperature. For the range $0\text{ }^\circ\text{C}$ to $961.78\text{ }^\circ\text{C}$, the reference function is

$$t_{90}/^\circ\text{C} = D_0 + \sum_{i=1}^9 D_i \left\{ \left[W_{ref} - 2.64 \right] / 1.64 \right\}^i \quad (8.3)$$

The constants, D_i , are given in table 8.1.

i	D_i
0	439.932 854
1	472.418 020
2	37.684 494
3	7.472 018
4	2.920 828
5	0.005 184
6	-0.963 864
7	-0.188 732
8	0.191 203
9	0.049 025

Table 8.1 - Constants used in ITS-90 reference equation

The reference equation is accurate to $\pm 0.000\ 13\text{ }^\circ\text{C}$. The calibration data for the PRTs used in the interferometer are given in table 8.2.

Channel	PRT	$R(0.01\text{ }^\circ\text{C}) / \Omega$	a
1	AJL1	100.006 69	-0.018 983 35
2	AJL2	100.001 51	-0.018 848 02
3	AJL3	100.001 86	-0.018 906 89
4	SP1	100.000 76	-0.018 765 43
5	AJL5	100.003 21	-0.018 926 23
6	SP2	100.009 14	-0.019 009 72
7	AJL7	100.007 51	-0.019 267 32
8	AJL8	99.993 67	-0.019 223 35

Table 8.2 - Calibration data for interferometer PRTs

The calibration data is stored in the computer program and is automatically used to calculate values of temperature, based on values of resistance measured by the resistance bridge. When measuring the temperature of a PRT, the program selects the PRT before waiting for the bridge to balance over the next 20 seconds or so. The computer program waits for the ‘balancing’ signal to be cleared, then waits until the temperature readings of the PRT are stable to within 1 mK over a few seconds. Thus no temperature measurements can be made if the temperature is changing rapidly.

8.4 STABILITY OF TEMPERATURES INSIDE CHAMBER

8.4.1 Measurements at 20 °C

Measurements of the temperatures inside the chamber show that the temperature control circuit works well, and controls the temperatures of the bars inside the chamber to $20\text{ °C} \pm 0.03\text{ °C}$, with resetability in this range after heating to 30 °C . The temperature control and stability are better than the $\pm 0.2\text{ °C}$ air temperature control of the room, as shown in figure 8.5. A typical drift rate for the air and bar temperatures is less than 2 mK per hour.

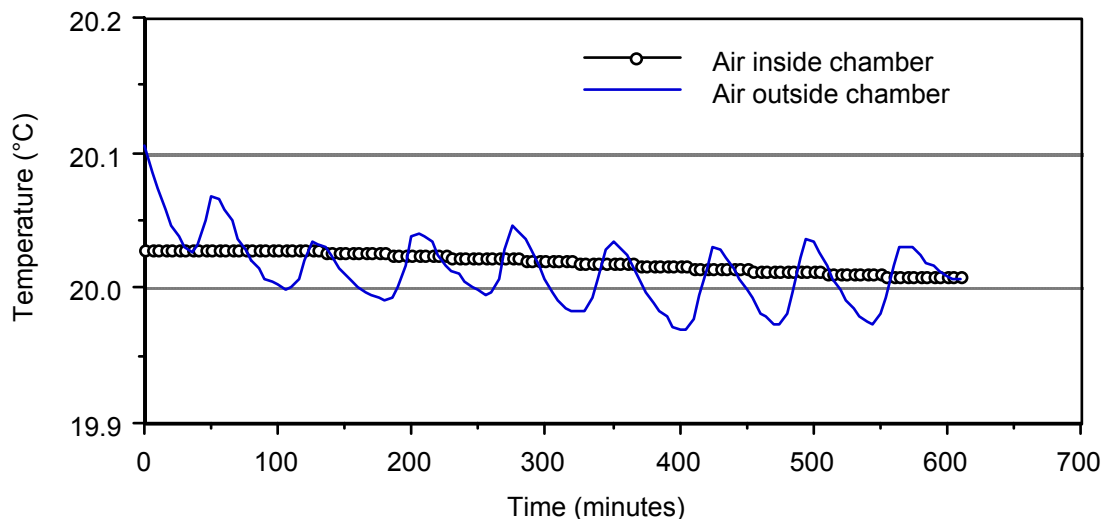


Figure 8.5 - Stability of air temperature inside chamber at 20 °C

Temperature gradients inside the chamber are also very small at 20 °C. The readings shown in figure 8.6 were taken with a 150 mm bar resting on PRTs 1 and 4, a 36 inch bar on PRTs2 and 5, and a 400 mm bar on PRTs 3 and 6.

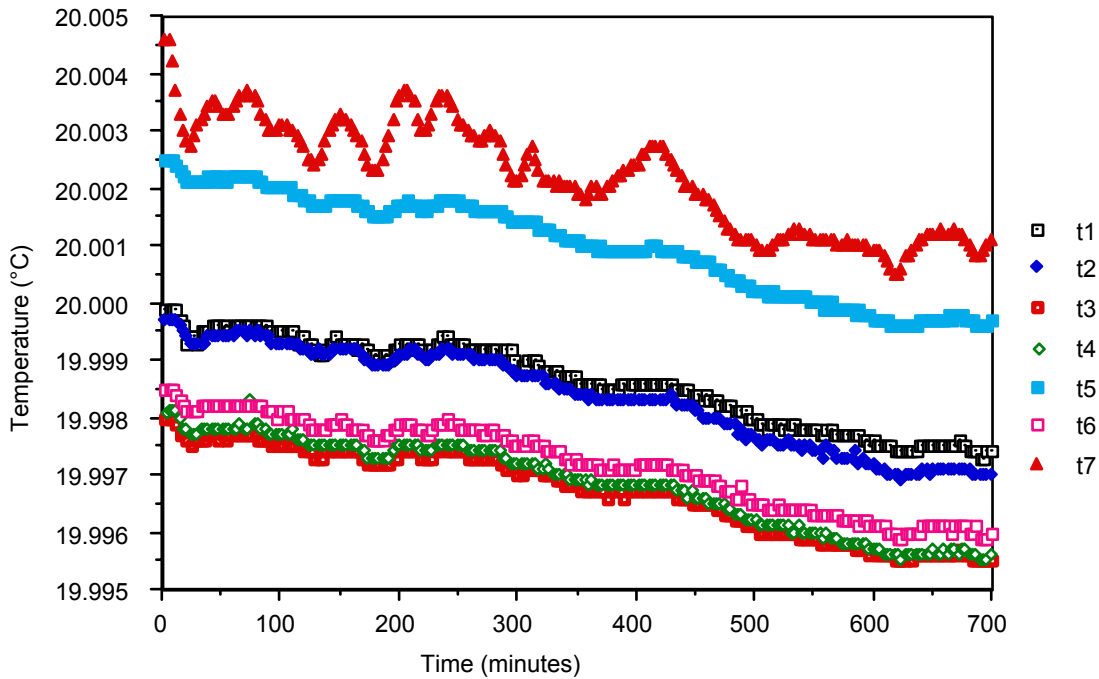


Figure 8.6 - Stability of bar and air temperatures at 20 °C

8.4.2 Heating from 20 °C to 30 °C

Normally, the temperature of the chamber is stepped over the range 20 °C to 30 °C in 2 °C increments when performing thermal expansion measurements. Each temperature step requires approximately 16 hours for the temperatures of the bars and the air to stabilise before measurements are made. This is usually performed overnight, allowing measurement the next day. Measurements are not performed until the temperatures are stable to within ± 1 mK over the time taken for measurement (approximately 2 minutes).

Normally, the PRT that controls the water circulator is placed in thermal contact with the baseplate of the interferometer. Tests have also been performed with the PRT placed inside the water bath of the circulator. As expected, the time required to heat the chamber was increased because the water temperature was stabilised at the set point temperature, rather than being raised higher, to provide faster heating. This is shown in figure 8.7.

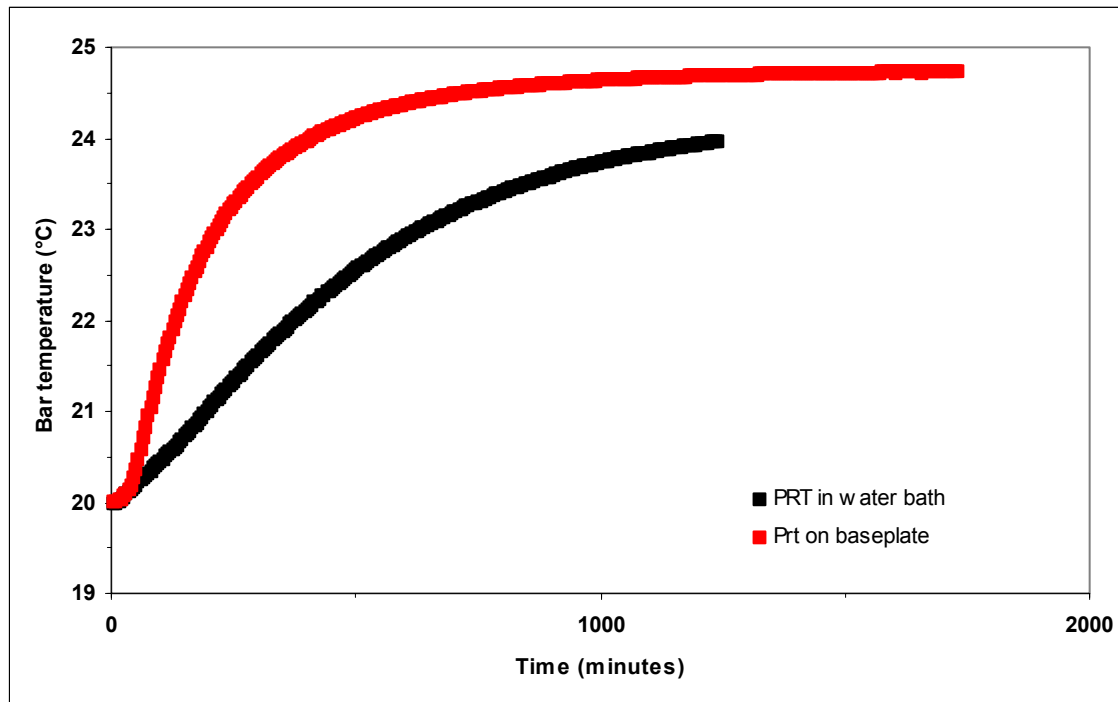


Figure 8.7 - Comparison of heating rates using PRT on baseplate or in water bath

As the temperature is raised, temperature gradients appear inside the chamber due to un-even heating. This leads to a variation in the temperature of the air along the path surrounding the length bar. This causes a temperature gradient in the length bar, with the hottest end being the one to which the platen is wrong.

The temperature gradient has been measured by attaching all PRTs inside the chamber to a 1000 mm length bar, except for the two PRTs which remained in the supports underneath the bar.

The temperature gradients of the air in the measurement path have been measured by placing 5 of the PRTs inside small heat sinks, and placing these in the air alongside a 36 inch bar, supported on the usual 2 PRT supports. The results are shown in figure 8.8, for a temperature of 25.76 °C.

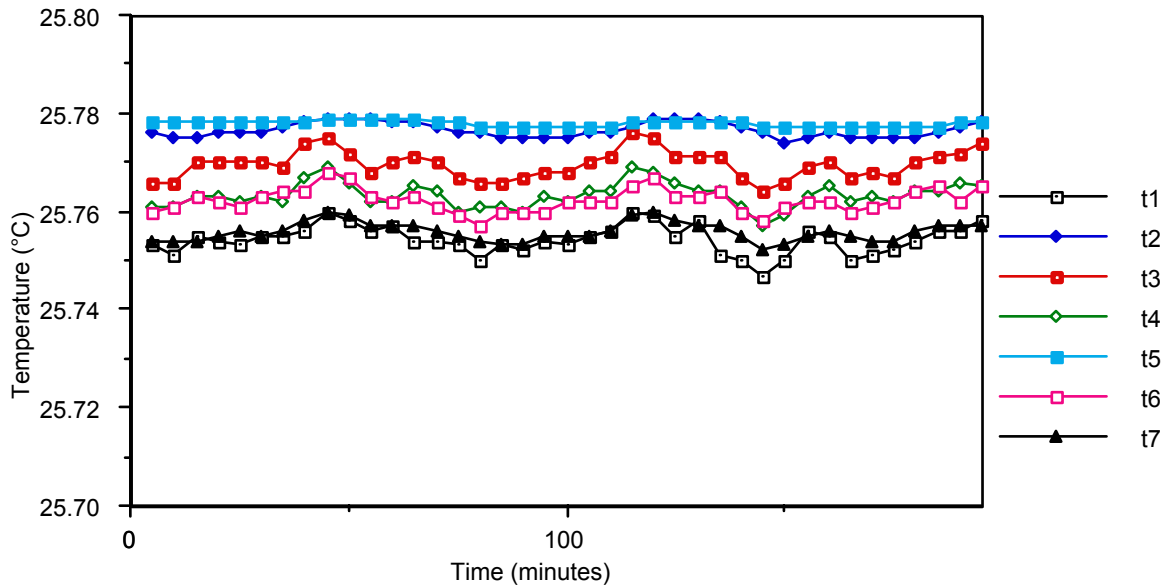


Figure 8.8 - Temperature measurements of air temperature gradients: t_2 & t_5 are the support temperatures, t_1 , t_3 , t_7 , t_4 & t_6 are air temperatures, in order from the unwrung end to the wrung end

8.5 CALCULATION OF THERMAL EXPANSION COEFFICIENTS

The linear coefficient of thermal expansion, α , is defined by equation (8.1).

$$\alpha = \frac{L_2 - L_1}{L_1(T_2 - T_1)} \quad (8.4)$$

where L_1 and L_2 are the lengths of the bar measured at temperatures T_1 and T_2 , respectively. Generally $T_2 > T_1$ and α is positive for steel, hence $L_2 > L_1$. Thus α may be measured by measuring the length of a bar at two known temperatures and then using equation (8.4). A more accurate value can be obtained by measuring at many temperatures and obtaining a set of temperature-length data pairs. This data is analysed as follows. Firstly, the temperatures are all referenced to 20 °C, *i.e.* 20 °C is subtracted from each temperature reading. A least-squares fit of a quadratic function is then performed. The fitted function is

$$L(T) = L_{20} + \alpha'T + \beta'T^2 \quad (8.5)$$

where T = Temperature - 20 °C, L_{20} = length of bar at 20 °C, α' = linear expansivity, β' = 2nd order non-linear expansivity, $L(T)$ = length of bar at T degrees above 20 °C.

The second order coefficient β' is included to take account of any non-linearity of the expansion. Generally β' is of the order of $\alpha'/1000$ in magnitude for length bar steel.

The required coefficients of thermal expansion α and β are obtained from the expansivities α' and β' by dividing by L_{20} . This gives

$$L(T) = L_{20}(1 + \alpha T + \beta T^2) \quad (8.6)$$

According to standard texts [7], α can be represented by $\alpha = a + bt + ct^2$ where a , b and c are constants, and t is the temperature. In this case, the value of α in (8.6) corresponds to a and β corresponds to b . The coefficient c is very small and over the temperature range encountered in normal laboratory conditions is completely negligible. For this thesis, equation (8.4) will be used to define α , and β will be considered as the departure from linear expansion, *i.e.* the variation of α with temperature.

8.6 ERRORS IN α AND β

A full error analysis of the calculated α and β values is possible by examining the errors of a least squares fit to data pairs, with errors in both variables, using Monte-Carlo techniques. However an order of magnitude estimate can be obtained from the usual theory of error propagation. This will be used to calculate the error in α . Second order β effects can be assumed to be negligible: it will be shown that these are in the 'noise' of the measurements. An order of magnitude analysis also gives more insight into what the main sources of error are.

8.6.1 Error propagation method - calculation of error in α and β

If α is calculated from (8.4), then the error $\Delta\alpha$ in the calculation of α is given by

$$(\Delta\alpha)^2 = \left(\frac{\partial\alpha}{\partial L_2} \Delta L_2\right)^2 + \left(\frac{\partial\alpha}{\partial L_1} \Delta L_1\right)^2 + \left(\frac{\partial\alpha}{\partial T_2} \Delta T_2\right)^2 + \left(\frac{\partial\alpha}{\partial T_1} \Delta T_1\right)^2 \quad (8.7)$$

where

ΔL_1 = error in measurement of L_1

ΔL_2 = error in measurement of L_2

ΔT_1 = error in measurement of T_1

ΔT_2 = error in measurement of T_2

Now

$$\frac{\partial \alpha}{\partial L_2} = \frac{1}{L_1(T_2 - T_1)} \quad , \quad \frac{\partial \alpha}{\partial L_1} = \frac{-L_2}{L_1^2(T_2 - T_1)} \quad (8.8)$$

$$\frac{\partial \alpha}{\partial T_1} = -\frac{L_2 - L_1}{L_1(T_2 - T_1)^2} \quad , \quad \frac{\partial \alpha}{\partial T_2} = \frac{L_2 - L_1}{L_1(T_2 - T_1)^2} \quad (8.9)$$

$$(\Delta \alpha)^2 = \left[\frac{\Delta L_2}{L_1(T_2 - T_1)} \right]^2 + \left[\frac{L_2 \Delta L_1}{L_1^2(T_2 - T_1)} \right]^2 + \left[\frac{\Delta T_2(L_2 - L_1)}{L_1(T_2 - T_1)^2} \right]^2 + \left[\frac{\Delta T_1(L_2 - L_1)}{L_1(T_2 - T_1)^2} \right]^2 \quad (8.10)$$

So far, the analysis is exact. Now use the substitution

$$\frac{L_2 - L_1}{L_1(T_2 - T_1)} = \alpha \quad (8.11)$$

The rest of the results will be exact, if α is correct.

$$(\Delta \alpha)^2 = \left[\frac{\Delta L_2}{L_1(T_2 - T_1)} \right]^2 + \left[\frac{L_2 \Delta L_1}{L_1^2(T_2 - T_1)} \right]^2 + \left[\frac{\Delta T_2 \alpha}{(T_2 - T_1)} \right]^2 + \left[\frac{\Delta T_1 \alpha}{(T_2 - T_1)} \right]^2 \quad (8.12)$$

To remove terms in L_2 , approximate $L_2 \sim L_1$. This is acceptable since there are no terms which involve $L_2 - L_1$.

$$(\Delta \alpha)^2 = \frac{1}{(T_2 - T_1)^2} \left[\frac{\Delta L_2^2 + \Delta L_1^2}{L_1^2} + \alpha^2 (\Delta T_2^2 + \Delta T_1^2) \right] \quad (8.13)$$

Thus $\Delta \alpha$ depends on the errors in the measurements of the temperatures and the lengths, and on the size of α and the temperature step between readings. This is an approximate result, which is exact if the value of α is known, and is not too large, *i.e.* for $L_2 \sim L_1$ to be valid. There is an important distinction to make when selecting contributions to ΔL_1 , ΔL_2 , ΔT_1 and ΔT_2 . Any terms which can be attributed directly to temperature error must not be included in the value for the length errors, even if they contribute a length uncertainty at either temperature, since this would include them twice in the error budget.

The value to use in this analysis for ΔL_1 is the uncertainty in length measurement at 20 °C, which is shown in chapter 10 to be approximately ($\pm 30 \pm 62 L_1$) nm. The value

of α is taken as $10.7 \times 10^{-6} \text{ K}^{-1}$. The uncertainty in T_1 is shown in chapter 10 to be $\pm 1 \text{ mK}$. The errors in T_2 and L_2 require further consideration.

The error in T_2 has two sources: the non-linearity of the horizontal temperature gradient in the length bar and the vertical temperature gradient across the length bar. A maximum value of the horizontal gradient has been obtained from measurements of the 1000 mm length bar. At $30 \text{ }^\circ\text{C}$, the departure from a linear-temperature gradient contributed a temperature measurement error (of the bulk mean temperature of the bar) of 5 mK . At the same temperature, there was a 1 mK temperature gradient across the vertical diameter of the bar, between the PRTs in the supports and those attached to the top of the bar. The magnitudes of these temperature gradients are temperature-dependent.

The sum of these contributions gives

$$\Delta T_2 = \pm 0.0006 (T_2 - T_1) \text{ K.}$$

The sources of error in the length measurement are as follows.

(1) Inaccuracy of the Edlén equations due to horizontal air temperature gradients between the sensor and the mean position along the length of the bar. This was measured as $25 \text{ mK m}^{-1} \text{ K}^{-1}$. This is length-dependent because the longer the bar, the further away the sensor from the ideal measurement position at the centre of the bar.

(2) Drift of the alignment of the interferometer. The alignment of the interferometer drifts as the optics are heated due to a differential expansion of the mirror mounts. This causes the reference and measurement beams to become slightly mis-aligned. Before any measurement is performed at a raised temperature, the beams are re-aligned. Further drift is expected to contribute an error of less than 1×10^{-9} per degree temperature excursion.

(3) Raised temperature inaccuracies of the Edlén equations. The use of the Edlén equations at raised temperatures is expected to result in a length measurement error of $1 \times 10^{-9} \text{ K}^{-1}$.

(4) The measurement will be subject to the other errors, encountered for measurements at $20 \text{ }^\circ\text{C}$. The value give above is $(\pm 30 \pm 62 L_1) \text{ nm}$.

The sum of these contributions gives

$$\Delta L_2 = 2(T_2 - T_1) \text{ nm} + 30 \text{ nm} + 62 L_1 \text{ nm} + 2.3 L_1(T_2 - T_1) \text{ nm.}$$

Substituting these into equation (8.13) gives the following errors for α .

Temperature Step $T_2 - T_1$ (°C)	1	2	3	4	5	6	7	8	9	10
Bar length L_1 (mm)										
100	0.430	0.220	0.150	0.110	0.089	0.075	0.065	0.058	0.053	0.048
200	0.230	0.120	0.078	0.059	0.048	0.040	0.035	0.031	0.028	0.026
300	0.170	0.084	0.056	0.043	0.035	0.029	0.026	0.023	0.021	0.019
400	0.140	0.070	0.047	0.036	0.029	0.025	0.021	0.019	0.018	0.016
500	0.120	0.062	0.042	0.032	0.026	0.022	0.019	0.017	0.016	0.015
600	0.110	0.057	0.038	0.029	0.024	0.020	0.018	0.016	0.015	0.014
700	0.110	0.054	0.036	0.028	0.023	0.019	0.017	0.015	0.014	0.013
800	0.100	0.052	0.035	0.027	0.022	0.019	0.016	0.015	0.014	0.013
900	0.100	0.051	0.034	0.026	0.021	0.018	0.016	0.014	0.013	0.012
1000	0.098	0.049	0.033	0.025	0.021	0.018	0.016	0.014	0.013	0.012
1100	0.097	0.049	0.033	0.025	0.021	0.018	0.015	0.014	0.013	0.012
1200	0.095	0.048	0.032	0.025	0.020	0.017	0.015	0.014	0.013	0.012
1300	0.094	0.048	0.032	0.025	0.020	0.017	0.015	0.014	0.013	0.012
1400	0.094	0.047	0.032	0.024	0.020	0.017	0.015	0.014	0.012	0.012
1500	0.093	0.047	0.032	0.024	0.020	0.017	0.015	0.014	0.012	0.012

Table 8.3 - Error in measured value of α (10^{-6} K^{-1})

8.6.2 Least-squares fit to data with errors in both coordinates

To obtain robust estimates of the errors in the α and β values obtained by least-squares fitting of a quadratic to the length - temperature data requires the adoption of an error analysis such as that proposed by Cecchi [8] (and subsequently corrections by Moreno & Bruzzone [9]). This technique uses the error propagation law and the canonical least-squares equations to estimate the variances in the calculated linear and quadratic terms. A curve-fitting algorithm based on this analysis has been developed by Ben Hughes at NPL for performing exactly the same analysis as required here, for the NPL Gauge Block Dilatometer.

The data given in § 9.6 for the thermal expansivity of a 900 mm bar is reproduced here. Six pairs of data corresponding to the measured length and temperature of the length bar were used as the data for a least-squares fit of a quadratic, using *Mathematica*. The results for the α and β coefficients and the length at 20 °C were:

$$L_{20} = 900.000\,570 \text{ mm}, \alpha = 10.633 \times 10^{-6} \text{ K}^{-1}, \beta = 8.6 \times 10^{-9} \text{ K}^{-2}$$

From the simple error analysis of the preceding section, the error in α was estimated to be $\delta\alpha = \pm 0.051 \times 10^{-6} \text{ K}^{-1}$, with $L_1 = 900 \text{ mm}$, $T_2 - T_1 = 2 \text{ °C}$ (the temperature step between readings).

The results of the curve fitting algorithm using the same data, but weighted according to the estimates of the errors in the temperature and length measurements, were:

$$L_{20} = 900.000\,572 \text{ mm}, \alpha = 10.631 \times 10^{-6} \text{ K}^{-1}, \beta = 8.8 \times 10^{-9} \text{ K}^{-2}$$

with estimated variances of $\delta\alpha = \pm 0.04 \times 10^{-6} \text{ K}^{-1}$, $\delta\beta = \pm 4 \times 10^{-9} \text{ K}^{-2}$. Thus the calculated values for the α coefficient differ by only $0.002 \times 10^{-6} \text{ K}^{-1}$, and the β coefficients by $0.2 \times 10^{-9} \text{ K}^{-2}$. The estimates of the length of the bar at 20 °C differ by only 2 nm. The error in the value of α was overestimated by the simple error analysis by $0.011 \times 10^{-6} \text{ K}^{-1}$ (22%). The close agreement is because the errors in the length and temperature measurements are small compared to the values of the measurements. Thus it appears ‘safe’ to use the simple analysis for estimating the error in the measured expansion coefficient. For measurements of expansion coefficient, it is sufficient to use a simple least-squares analysis to calculate the length of the bar and its expansion coefficient, given the size of the other uncertainties (see chapter 10).

8.7 EXAMPLE OF THERMAL EXPANSION MEASUREMENT

As an example of a thermal expansion measurement, a 1000 mm length bar was measured over the temperature range 20 °C to 30 °C. The data were analysed in *Mathematica* and plotted in figure 8.10.

Bar temperature (°C)	Bar Length (mm)
20.009	1000.003 679
21.896	1000.023 850
24.719	1000.054 058
27.727	1000.086 357
30.034	1000.111 151

Table 8.4 - Measured thermal expansion data for a 1000 mm length bar

Length - 1000 (mm)

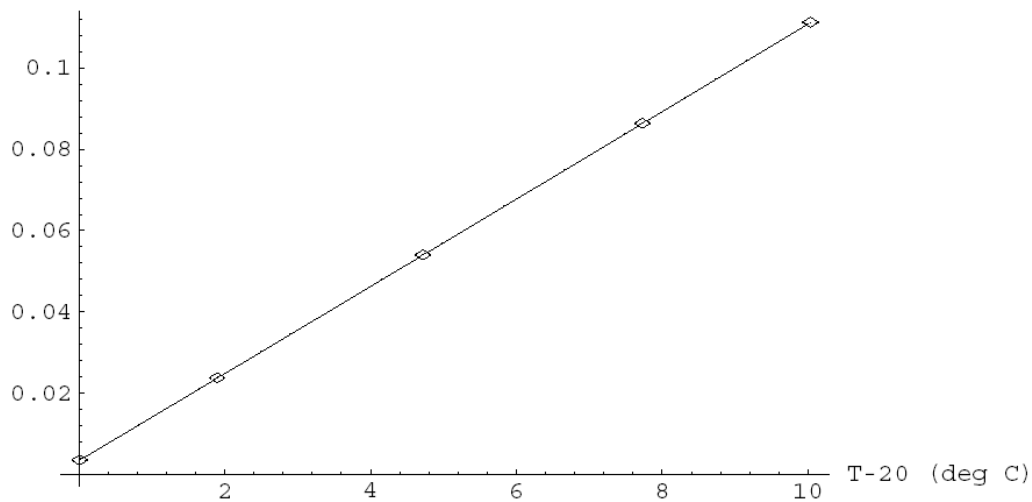


Figure 8.9 - Least squares quadratic fit to thermal expansion data for 1000 mm bar

After least squares fitting, the following coefficients were found:

$$L_{20} = 1000.003\,580 \text{ mm}, \alpha = 10.678 \times 10^{-6} \text{ K}^{-1} \text{ and } \beta = 4.2 \times 10^{-9} \text{ K}^{-2}$$

Using these coefficients, the agreement with the actual measured lengths at different temperatures ranges from 2.7 nm at 20.009 °C to 4.7 nm at 30.034 °C.

Further examples of thermal expansivity measurements can be found in chapter 9.

REFERENCES FOR CHAPTER 8

- [1] International Standard ISO 1 (1931) (Geneva: International Organisation for Standardisation)
 - [2] Rusby R L, Hudson R P, Durieux M, Schooley J F, Steur P P M & Swenson C A Thermodynamic basis of the ITS-90 *Metrologia* **28** (1991) 9-18
 - [3] British Standard BS 4311(1993) (London: British Standards Institution)
 - [4] Thermofoil™ heaters, Minco Products Incorporated, Minnesota USA
 - [5] Celotex™ Thermal sheathing: glass-fibre reinforced rigid polyisocyanurate foam faced on both sides with aluminium foils, Celotex Ltd., Ealing, London
 - [6] German Standard DIN 43760 (1980) (Berlin: Deutsches Institut für Normung e.V.)
 - [7] Kaye G W C & Laby T H *Tables of Physical and Chemical Constants* 15 edn (1989) (Harlow, Essex: Longmans)
 - [8] Cecchi G C Error analysis of the parameters of a least-squares determined curve when both variables have uncertainties *Meas. Sci. Technol.* **2** (1991) 1127-1128
 - [9] Moreno C & Bruzzone H Parameters' variances of a least-squares determined straight line with errors in both coordinates *Meas. Sci. Technol.* **4** (1993) 625-636
-